Accepted Manuscript

Comparison of expert, deterministic and Machine Learning approach for landslide susceptibility assessment in Ljubovija Municipality, Serbia

Jelka Krušić [1], Miloš Marjanović [1], Mileva Samardžić-Petrović [2], Biljana Abolmasov [1], Katarina Andrejev [1] and Aleksandar Miladinović [3]

[1] Faculty of Mining and Geology, University of Belgrade, Belgrade, Serbia

[2] Faculty of Civil Engineering, University of Belgrade, Belgrade, Serbia

[3] Energoprojekt Holding, Belgrade, Serbia

Landslide Susceptibility Assessment is becoming a very productive research area, wherein different modeling approaches are practiced to delineate zones of the high-low likelihood of landslide occurrence. However, there is no strong consensus on which approach is the most adequate. The reason behind the lack of the general view on the performance of different approaches could be partially explained by the particularity of each study. To evaluate the efficiency of different approaches they need to be applied under the same conditions for the same study area. Herein, we examined three different approaches, including expert, deterministic and Machine Learning, on the example of Ljubovija Municipality in western Serbia. The study area has been known as susceptible to landslides, and represents good ground for assessing the chosen methods. It is represented by complex geology, prone to landslides that are commonly hosted in thick weathering crust of Paleozoic formations, composed of schists and meta-sediments. Under extreme triggering conditions, such as the one that unfolded in May 2014, these thick weathering crusts saturate, and give way to a variety of landslide and flash-flood processes that we will be focusing on in this study. The application of the expert-approach, through Analytical Hierarchy Process provided a rough assessment map. The deterministic model, which couples simple infinite slope and hydrological model, provided us with lower quality results, when compared to the expert-based one. This could be explained by the assumptions used in the model are too simplistic to generically model a wide range of landslide typology. Finally, Machine Learning approach, using the Random Forest algorithm, provided significantly better results and showed that it can cope with versatile landslide typology over larger scales. Its AUC performance is about 0.75 which is considerably outperforming the AUC values of the other two models, which were up to 0.55, *i.e.* at the level of random guess.

1. Introduction

There are various approaches to Landslide Susceptibility Assessment (LSA), including expert-driven, deterministic, statistic and Machine Learning methods (Guzzetti et al., 1999). Which of them will perform better in a particular case is difficult to determine beforehand, so trial-and-error and comparative studies are always necessary. Reasons that underpin the complexity of this topic are many: quality of input data, suitability of the model, but one of the main reasons lies in the nature of landslide phenomena itself. For instance, the massive rainfall event can simultaneously trigger various types of landslides, which can be different in their mechanisms, size, character, depth, etc. It is, therefore, difficult for any LSA approach to cope with all these circumstances. Herein, one such case was addressed, linked to a heavy rainstorm and subsequent flooding and massive landsliding that occurred in Serbia in May 2014. In particular, it addresses Ljubovija Municipality in western Serbia, as one of the areas that suffered the heaviest aftermath, in respect to the number of landslides and total damage, but also in respect to a very diverse landslide typology: shallow and deep-seated, rapid and slow, reactivated and newly-formed. It was therefore convenient to use the area of Ljubovija for testing various LSA approaches and comparing their performance, fulfilling the principal objective of this study. Three different approaches were applied and compared:

- for expert-driven or heuristic approach – Analytical Hierarchy Process (AHP) was used
- for deterministic or physical approach – Stability Index (*SI*) modelling was implemented
- for Machine Learning data-driven approach – Random Forest (RF) algorithm was implemented.

Heuristic methods are mainly qualitative and subjective, as they depend on the judgment of decision makers (experts) in particular research area. The most common heuristic approach is based on analyzing landslide inventory to identify sites of similar geological and geomorphological properties. Many authors do not recommend the use of heuristic methods for hazard, but only for susceptibility zoning (Fell et al., 2008; Cascni, 2008; Barredo et al., 2000; Ercanoglu et al., 2008). The reason for this is that the results are partly subjective, and depend on the experience of experts, which implies insufficient knowledge and sometimes generalization of the results in a particular area (Atkinson and Massari, 1998; Ayalew and Yamagishi, 2005; Yalcin, 2008; Yilmaz, 2009). On the other hand, it

is generally accepted that heuristics could and should be used for preliminary levels of research-regional studies (Soeters and van Westen, 1996; Fell et al., 2008; Guzzetti et al., 1999). Some methods include ranking and weighting, which implies semi-quantitative approach (Ayalew and Yamagishi, 2005). Analytic Hierarchy Process (AHP), first time used by Saaty 1980, is one of the semi-quantitative methods that allows subjective as well as objective factors to be considered in the decision-making process. Successful examples of AHP implementation were reported by numerous researchers, but the main impression remains that it is more suitable for preliminary assessment on regional scales (Komac et al., 2006).

Deterministic modeling on regional scales is difficult due to a number of reasons: amount and sampling density of required physical parameters, which can be very costly, as well as the appropriateness of applied geometrical and physical modeling assumptions to the given case study. The number of physical and geometric parameters is therefore reduced, at the expense of simplifying the model. Ultimately, only the simplest Limit Equilibrium (LE) slope stability methods comply, *e.g.* infinite slope model, where geometry and landsliding physics are trivial. The LE models are usually coupled with simplified hydrological models. The impression is that deterministic methodology in LSA is rather limited and rounded. The only differences that are practiced come down to the variation of coupled hydrological models or small adjustments or extensions to the original LE assumptions of infinite slope model in regional assessment (Montrasio and Valentino 2016). The pioneering work in deterministic LSA was performed by Montgomery and Dietrich, 1994, where the general LE principle is implemented through the Stability Index (SI), coupled with a transient steady-state groundwater flow model. There were further attempts to sophisticate the LE conditions by introducing additional forces, or dimensionless factors (Pack et al., 2001), involve stochastics through input data distribution estimations (Pack et al., 2001), but mostly by including more complex coupled hydrological model: 3D-Richards equation; temporal, frost, and unsaturated terrain effects (Rigon et al., 2006; Endrizzi et al., 2013; Oh and Lu, 2015). Most of these researchers further emphasized that deterministic approach is more apt for local modeling, *i.e.* site-specific scales than regional, whereas regional scales face various limitations. Considerable generalization of landsliding mechanism is therein always needed, entailing that only shallow slides, triggered solely by rainfall discharge, comply with regional assessment. Partly, this was the case with landslides triggered in Ljubovija in May 2014, except that there were many flows in combination with shallow slides, so the applicability of discriminant modeling is relatively sound for the case of Ljubovija.

The capability of the ML techniques to learn and derive patterns of the phenomena of interest by exploring unknown relations between considering

casual/conditional factor and the variable of interest has made these techniques very popular in many various fields of science, including the LSA. Many research studies have already successfully applied various ML techniques for LSA, such as Decision Tree (DT), Neural Network (NN), Support Vector Machine (SVM) and Logistic Regression (LR) (Lifeng and Youshui, 2006; Marjanović et al., 2011; Pradhan, 2013) and more recent RF. As a relatively new ML technique, RF, which generates a model by combining the results of a set of simpler DT-based models, received increasing attention in the LSA community (Catani et al., 2013; Goetz et al., 2015; Trigila et al., 2015; Vorpahl et al., 2012). One of the first published researches, that addresses the application of RF for the LSA, was performed by Vorpahl et al. (2012). In order to model LSA, they used five historical landslide inventories and seven terrain attributes derived from a Digital Elevation Model (DEM). They compared eight different techniques and concluded that RF and Boosted Regression Tree (BRT) had better performance compared to Generalized Linear Models (GLM), General Additive Models (GAM), Multivariate Adaptive Regression Splines (MARS), NN, DT (CART) and Maximum entropy method (MEM). Goetz et al. (2015) compared the performance of six various statistical and ML techniques for LSA: GLM, GAM, weights of evidence (WOE), SVM, RF, and Bootstrap aggregated classification trees with penalized discriminant analysis (BPLDA). They conducted the study using three study areas and 11 terrain attributes derived from DEM, as predictor variables. The derived results also suggested that the RF was one of the techniques with best prediction performance. Trigila et al. (2015) created LR and RF-based LSA models, using highly urbanized study area and in addition to terrain characteristic derived from DEM they used Distance to stream, Lithology, Land use/land cover, Agricultural terraces, and Wildfires as predictors. They found that both techniques equally provide excellent results. Considering some of the advantages of RF compared to other ML techniques (such as that RF does not overfit due to the Law of Large Numbers and its capability to handle scarce attributes (Breiman, 2001)) and that in most of the literature related to the LSA, RF technique was identified as one of the best performings, this technique was selected to represent Machine Learning data-driven approach for this research the case study.

2. Methods

Herein, all three modeling methods, *i.e.* expert-based, deterministic, and Machine Learning, will be elaborated, as well as the principle of their evaluation against the existing landslide inventory, and related evaluation metrics.

2.1. Expert method – Analytical Hierarchy Process (AHP)

Analytic Hierarchy Process (AHP) is one of the most popular Multi-Criteria Decision-Making (MCDM) tools for formulating and analyzing decisions (Saaty, 1980; Ishizaka and Labib, 2011). This methodology calibrates the numeric scale for the measurement of quantitative as well as the qualitative influence of separate attributes on the phenomena at hand. The scale of influence ranges from 1/9 for "least valued than 9", to 1 for "equal", and to 9 for "absolutely more important than" covering the entire spectrum of the comparison (Vaidya and Kumar, 2006). Multiple criteria decision problem is first broken down into its component parts of which every possible attribute is arranged into multiple hierarchical levels. The AHP consists of three main operations, including hierarchy construction, priority analysis, and consistency verification (Ho, 2008). This approach is widely used in the assessment of landslide susceptibility (Komac, 2006; Marjanović et al., 2011; Yalcin, 2008; Pourghasemi et al., 2012). The implementation of AHP methodology in the assessment of landslide susceptibility firstly requires finding of interdependencies between most important influential attributes, in this case: engineering geological units, slope, elevation, distance from hydrogeological borders, stream distance, land cover, aspect, and erodibility. It is highly recommended to normalize the values of input attributes and classify them into a specific number of classes (*e.g.* herein 1–5 class range was used, meaning that 1 is the least likely to host landslides and 5 is highly likely to host landslides). AHP principle further implies generation of a comparative matrix of selected attributes with the 1–9 scale of influence. It is inversely symmetric ($a_{ij} = a_{ji} = 1$) in respect to the main diagonal. Reclassified and ranged attributes (A_i), with their weights (W_{Ai}), give final impact on susceptibility model (LSM). The sum of the weights of all the parameters is equal to 1, or 100% (Saaty, 1980; 1987; Saaty and Vargas 2001). Consistency of attribute comparison is defined by Consistency Ratio – CR (Bhushan and Rai, 2004; Subramanian and Ramanathan, 2012; Saaty, 1980). This final operation controls the comparison judgment. Comparisons made by AHP method are subjective, and some inconsistency is tolerated. Consistency Index, *CI*, is calculated as:

$$CI = (\lambda_{max} - n) / (n - 1) \tag{1}$$

where λ_{max} is the maximum weight of the judgment matrix and n is the number of attributes. Accordingly, ($\lambda_{max} - n$) can be considered as a measure of the degree of inconsistency, which is normalized with $n - 1$ (Malczewski et al., 1997). The next step is to calculate Consistency Ratio, *CR*:

$$CR = CI / RI \tag{2}$$

where *RI* is the consistency index of a randomly generated pairwise comparison matrix, that depends on the number of criteria being compared. Saaty and

Vargas (2001) suggest the value of *CR* should be less than 0.10. If the values are above 0.10 revision of the judgment in the matrix is required.

2.2. Deterministic method – Stability Index (SI)

Stability Index (*SI*) concept consists of a typical slope stability model, coupled with a simple hydrological triggering model. Slope stability model is reduced to infinite slope geometry with simple Limit Equilibrium conditions, wherein slip surface is parallel to the topographic slope θ, the model is irrespective to the soil thickness, cohesion and pore pressure are canceled by soil weight to become unitless variables, effective stress Coulomb-Mohr's failure criteria is in power. General slope stability principle implies the static balance of driving and resisting forces that act on a slip surface. Their ratio is represented by the *Factor of Safety* (*FS*), which is further coupled with the triggering model by introducing boundary conditions of soil transmissivity vs. rainfall discharge *T/R*, wherein the stationary flow under steady-state conditions is assumed. Subsequently, stochastics is introduced into *FS* by ranging unit weight γ_{soil}, cohesion c_{soil}, friction angle φ_{soil} and transmissivity *T*, using uniform min/max distribution, to simulate the worst and best-case extremes (Eq. (3)). When *T/R* flux is maximal and strength parameters (c_{soil} and φ_{soil}) are at their lowest (assuming that water to soil weight ratio *r* is constant over designated rock unit) the worst-case extreme implies that *SI* will equal FS_{min}, and all areas with $FS_{min} > 1$ will be unconditionally stable, whereas values bellow 1 imply failure with appropriate level of probability. On the other hand, best-case extreme considers minimal *T/R* flux and highest strength parameters, wherein all areas with $FS_{max} < 1$ will be definitively unstable (*SI*=0), whereas those with values greater than 1 will also have some low probability to fail. All intermediate *FS* values with some probability of failure ($FS_{min} \leq 1$ and $FS_{max} \geq 1$) are further depending on slope angle θ and discharge area *a*, variables that are available for calculation for wider, regional scale areas in GIS. In general, the lower the *SI* index is, the lesser the stability and vice-versa. Herein, the modeling was performed in MapWindow via extension SINMAP – Stability Index MAPping (Pack et al., 2001).

$$FS = \frac{c_{soil} + cos\theta \left(1 - min\left(\frac{Ra}{Tsin\theta}, 1 \right) r \right) tg\varphi_{soil}}{sin\theta} \qquad (3)$$

2.3. Machine Learning method - Random Forest (RF)

RF is a relatively new ML technique, proposed by Breiman (2001), which has already achieved wide popularity in the Geoscience community with solving

various classification and regression problems. In this study, the spatial phenomenon of landslides is considered as a classification problem, with binary target variable l_i (1 = the location i is occupied with a landslide or 0 = not occupied with landslide). The main goal of the RF technique is to find the classification function, $c_i(a_1, a_2, ..., a_j) \rightarrow l_i$, which maps landslide and non-landslide class at a particular location. Consequently, each location defined by 30×30 m grid cell is presented as an instance c_i, which contains corresponding values of all conditioning factors a_j (factor such as: slope, erodibility, lithology, distance from hydrogeological borders, stream distance, aspect, land use elevation, …) and a landslide l_i as a target variable to be classified.

After defining the proper dataset which represents the entire study area as a set of instances $\{(c_i, l_i)\}$, $i = 1, …, 387,207$, the next step was to create two sub-datasets, for *training* and *testing*. The subset of the dataset used for finding the classification function, *i.e.* the relationship between the attributes and a landslide class is called the *training dataset*. The second subset, *testing dataset*, is independent of the *training dataset*. It was used to validate the obtained RF-based model by comparing the model classification outcome and real information of landslide. In order to provide a more informative *training dataset*, considering the relatively small number of instances which represent the landslide areas (1,475 instances, 0.38% of entire study area), the following sampling procedure proposed by Marjanović et al. (in press) was performed. A half of all instances which represent landslides were randomly selected as training landslide samples, ensuring that they are distributed across all landslide polygons from the inventory, with considering the size of each landslide polygon. The same number of training samples was selected as non-landslides, ensuring that they are distributed across all previously defined polygons (polygons were delineated on the basis of landslide expert judgment on which locations are highly unlikely to host landslides, such as ridge-lines, compact rocks, and flat surfaces).

Using this sampling strategy, both classes (landslide - 1 and non-landslide - 0) are equally represented, avoiding the possibility that the RF model can be affected by the majority classes, which in this study were the locations without landslides. The rest of the instances that have not been sampled for *training dataset* were used in the *testing dataset*. *Training dataset* contained 1,474 instances, 737 instances with landslides and 737 instances without landslides, whereas *testing dataset* contained 385,733 instances, 738 instances with landslides and 384,995 non-landslide instances.

The next step was to build the RF-based model. Generally, using *training dataset* RF generates a model by combining the results of a set of simpler decision trees (DT) based models (Fig. 1). Each DT in RF (Fig. 1) is constructed over a new subset of *training* dataset that contains randomly selected p

($p < 1,474$) instances of the initial *training dataset.* Furthermore, each DT in RF is grown using methodology proposed by Breiman (1984), *i.e.* by selecting attribute among q ($q < M$, $M =$ number of all considering attributes) randomly selected attributes, not among all considering attributes, as is usually done in DT.
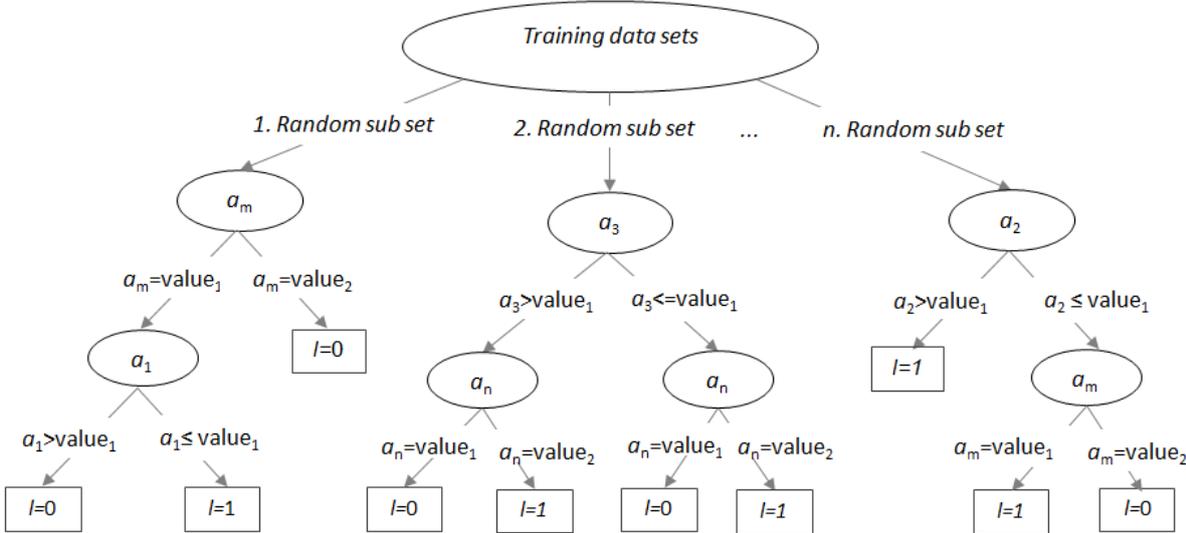

Figure 1. Schematics of the Random Forest implementation.

Finally, a RF obtains a classification outcome from each DT, and then further classifies using majority class for each instance or using the defined threshold of class 1 (landslide) probability.

The efficient application of most ML techniques requires selection of an optimal combination of function parameters, which are in the case of RF two parameters, the number of DT in the forest and the number of randomly selected factors that will be considered per each node in the DT. These parameters were found in the process of cross-validation in which a model is trained on a portion of the training dataset and validated on the remaining part, so that fitting parameters are optimized only over training instances.

Validation was performed on the testing dataset by comparing the models' outcomes with real information on landslides using the several validation measures: true positive rate (TPrate), false positive rate (FPrate), true negative rate (TNrate), false negative rate (FNrate) and Area Under Receiver Operating Characteristic Curve (AUC) (Bradley, 1997).

3. Case study area and data

The territory of the Municipality of Ljubovija is located in the western part of Serbia. It covers an area of 331.47 km² with a population of 3,929. The wider area can be characterized with moderate-continental to continental climate (Fig. 2). The Drina River and its valley dominate the landscape, together with its tributaries. The right side of the valley is quite steep, and exposed to slope processes: weathering, deluvial processes, gulling, landslides, and flash-floods. One of the longest tributaries is The Ljuboviđa River, which is known for its torrential character. In terms of the relief, the territory is predominantly hilly and mountainous. The highest peak is Tornička Bobija (elevation of 1,268 m), while the lowest part is the valley of The Drina River in the coastal area (158 m). The relative elevation difference between is 1,110 m, with an intermediate slope angle around 18°, but it is apparent that the terrain is mostly steep, with a maximum slope angle of 65°.
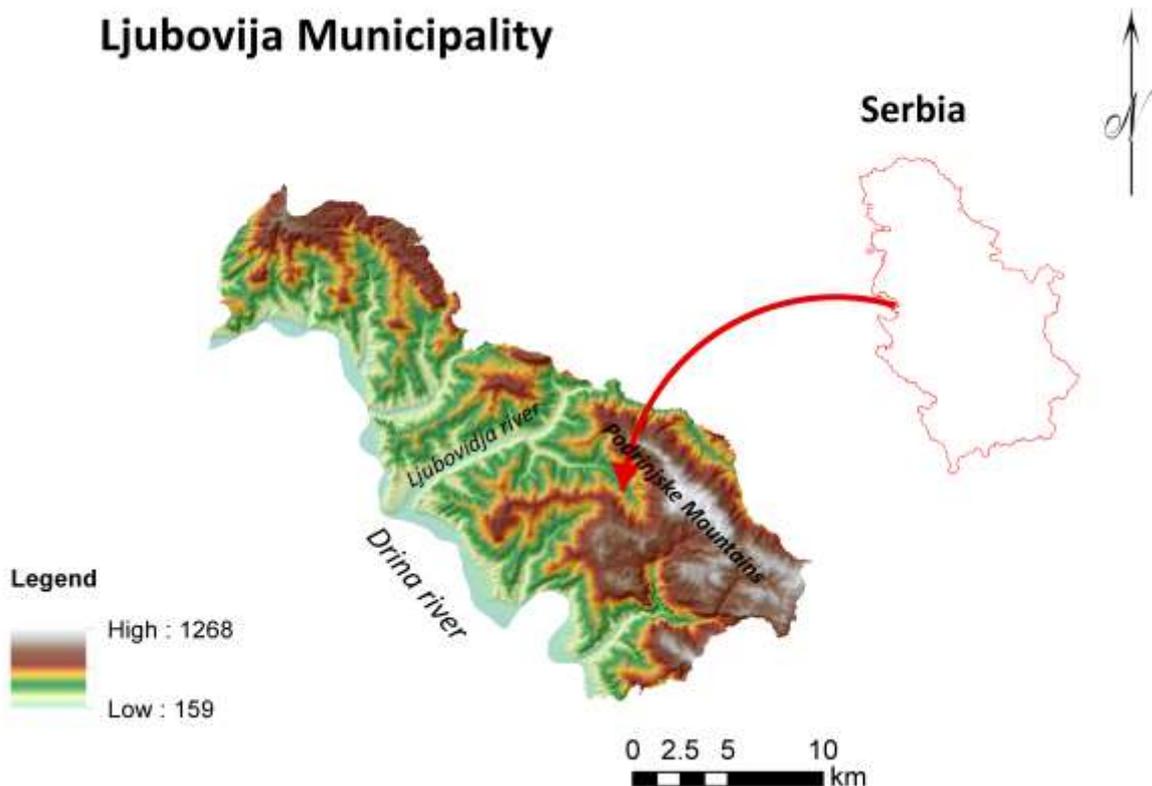

Figure 2. Geographical position and relief map (DEM 30 m resolution) of Ljubovija Municipality.

Regarding the geological settings, most of the terrain consists of Paleozoic formations (quartz sandstones and shales of lower crystallinity - phyllites and slates), Triassic formations (massive and plate crystalline limestones, dolomites, dolomite limestone), Jurassic formations (conglomerates, claystones and

serpentinites) and Quaternary deposits (deluvial-proluvial and alluvial sediments). Depending on the thickness of the weathering crust, different types of landslides could be expected to occur. It is typical that landslides hosted in the weathering crust mobilize after saturation, preceded by continuous rainfall input or a heavy rainfall, such as the one that took place in May 2014. During this event, maximum 72 h precipitation in the entire Serbia was recorded in this region, exceeding 200 mm. For comparison, the average amount of annual rainfall for the reference period (1981–2010) was 786.96 mm, while in 2014, in extreme conditions, it exceeded 1,249.98 mm. The average sum by a month in May for the reference period is 70.7 mm, and in May 2014 that sum was 234.5 mm, respectively 214.95% more than average. These conditions led to triggering of many new, and reactivating some of the suspended landslides. There were 271 landslides registered by remote sensing, and 70 landslides mapped in the field (Marjanović et al., 2016). Approximately, a half of all landslides are active landslides, and only 2% are stabilized or dormant (http://geoliss.mre.gov.rs/beware/).

4. Input data

Landslide inventory map that shows the location of discernible landslides is essential in landslide susceptibility mapping and hazards modeling (Dahal and Hasegawa, 2008; Pourghasemi et al., 2012). The total of 271 landslide occurrences inventoried across the entire study area, with the approximate size ranging from 15 m² to 143 780 m². As for the landslides recorded in the field, 49% were identified as active, 46% as suspended, and 5 % of landslides as inactive (stabilized, temporally dormant). During the initial rasterization of the inventory at 30 m resolution, these 271 occurrences were represented by only 213 30x30m landslide pixels, which was insufficient for modeling and evaluation. Thus, a 5 m buffer zone around each landslide was also considered as a landslide area, which increased the total number of landslide pixels to 265.

In order to assess susceptibility, as a spatial likelihood of occurrence of landslide events, it is necessary to determine landslide conditioning factors. The preparatory variables which make the slope susceptible to failure without initiating it, and thereby tending to put the slope in a marginally stable state, are usually considered constant, regarding the life of the landslide process, which is sometimes measured in decades. Three groups of attributes were considered, *i.e.* morphologic, geological and environmental.

Morphologic attributes

A Digital Elevation Model (DEM) is representing the terrain and it has been used to derive various morphometric parameters which influence slope instability. A DEM of the study area with 30×30 m cell size was generated using data from the Republic Geodetic Authority of Serbia. Adopted resolution was the optimal considering the fact that for regional LSA, 30 m cell resolution is enough detailed for DEM and the grid size is proper and compatible with other data sources, for example, Engineering Geological map at 1:300,000 scale. Morphometric thematic data layers such as slope, aspect, and elevation were compiled based on DEM.

Slope (A_2) – The main parameter of the slope stability analysis is the slope degree (Lee and Min 2001), and it is very commonly used in the landslide susceptibility studies (Lee, 2005; Yalcin, 2008; Nefeslioglu et al., 2008). Greater angles propose higher instability of the slopes and vice-versa, but with restriction to a particular rock type (*e.g.* solid rocks are expected to be stable even in steep slopes, while slopes in clay do not need a steep angle to host instability). The most of the landslides were located in range with an inclination of 10–20° (Fig. 3a).

Slope aspect (A_7) –This attribute (Fig. 3e) represents spatial exposure of the ground element to diurnal solar path and it ranges from 0° to 360°. Slope instabilities are affected by slope aspect because it is associated with the insolation which influences physical-mechanical decomposition of rocks, and moisture in the soil, which is important for landsliding (Suzen and Doyuran, 2004; Komac, 2006). It is assumed that northern and eastern slopes are the most inconvenient for stability (highest water retention and the thickest weathering crust), while the southern and western are the most favorable, due to different degrees of insolation.

Elevation (A_3) – Elevation is another feature physically related to landslides since potential energy is increasing with altitude, and thereby contributes landsliding. It is represented by DEM (Fig. 2).

Distance from the stream (A_5) – This attribute was generated from a digitized hydrography (Fig. 3c). Distance to stream has an influence on slope stability, due to the fact that deformation and failure processes develop regressively upslope under the vertical and lateral influence of the linear erosion of streams. Landslide occurrences along streams are often because streams are eroding and undercutting foot of the slope, and saturating its lower parts (Dai et al., 2001; Saha et al., 2002). In this respect, it is assumed that areas closer to the stream lines are more prone to instabilities than remote ones, thus landslide susceptibility decreases with distance from the local watercourse.

Geological attributes

Engineering geological units (A_1) – Different lithological units have essentially different physical-mechanical behavior and therefore different impact on slope stability. These were aggregated based on the engineering geological criteria into units of similar genesis and physical-mechanical properties (Fig. 4). This data was acquired from the engineering geological map of the study area at 1:300,000 scale. The landslides occurrence is likely in crystalline metamorphic rocks, which typically have a thick weathering crust, as well as softer lacustrine sediments. Flysch and ultramafic formations also hosted some occurrences, but to a much lesser degree.

Distance from hydrogeological borders (A_4) – This is a parameter that was introduced to emphasize the influence of hydrogeological boundaries on the landsliding process and the rate of change of hydrogeological function between adjacent rock masses (Fig. 3b). Zones closer to the boundary are more susceptible to landslide occurrence, which was confirmed by the field research.

Erodibility (A_8) – attribute was calculated from A_1 and A_6 according to Gavrilović (1971) methodology (Fig. 3f). Greater potential of erodibility is tightly related to landslidng process. Directly, landslides themselves are caused by erosional processes, and indirectly, landslides tend to develop along linear features such as gullies or ravines.

Environmental attributes

Land use (A_6) - This thematic attribute was obtained from CORINE Land cover 2012 data (Fig. 3d). Vegetated areas decrease the susceptibility to landsliding due to the increased root cohesion. Water retention is also greater in vegetated than bare surfaces, which is another stabilizing aspect. The land cover does not play a vital role during rapid and intense rainfall events, but they can be of importance for the long-term accumulation of water in soil (Yalcin et al., 2011).

Deterministic modeling approach involves more localized data. First, the samples are taken *in-situ*, and then used for a set of laboratory tests to obtain standard geotechnical parameters (bulk density, friction angle, cohesion, etc.) per each geological unit. Subsequently, these are generalized (extrapolated within the 30 m gridded rasters) over wider areas of presumably similar characteristics, called engineering geological units. The most important parameters to characterize an EG unit included unit weight, cohesion, friction angle, and hydraulic conductivity. Sampling and testing over wider areas would be very costly, which is why these parameters had to be estimated, based on previous research and generally suggested values (Fell et al., 2008). The EG units and their related parameters are outlined in Fig. 4, while Tab. 1 shows their values.
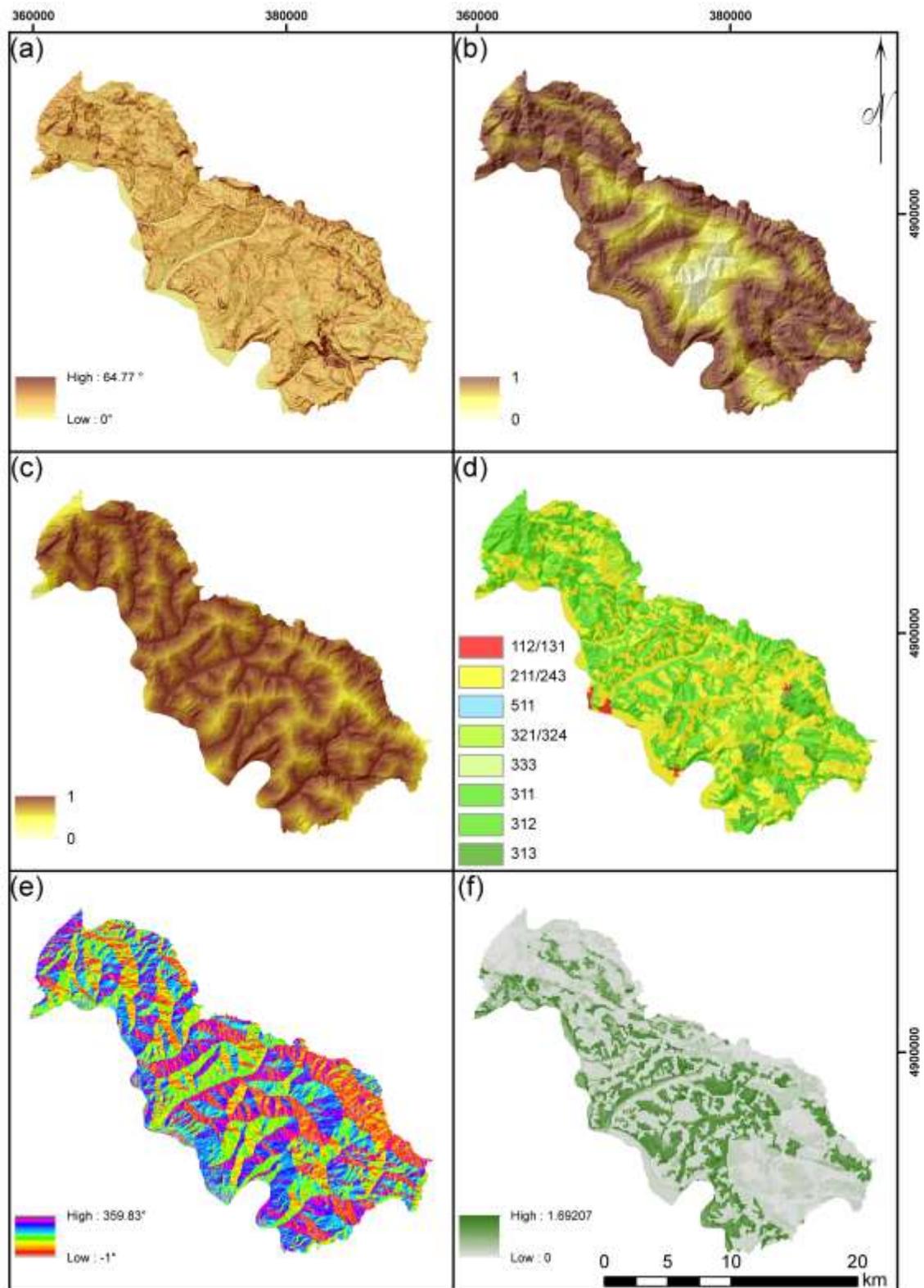
Figure 3. Input attributes (*a*) A_2 Slope, (*b*) A_4 Distance from hydrogeological borders, (*c*) A_5 Stream distance, (*d*) A_6 Land use (112/131-artificial surfaces; 211/243-agricultural areas; 311/313-forests; 321/324 - scrub and herbaceous vegetation association; 333-sparsely vegetated areas; 511-water courses) (*e*) A_7 Aspect, (*f*) A_8 Erodibility.
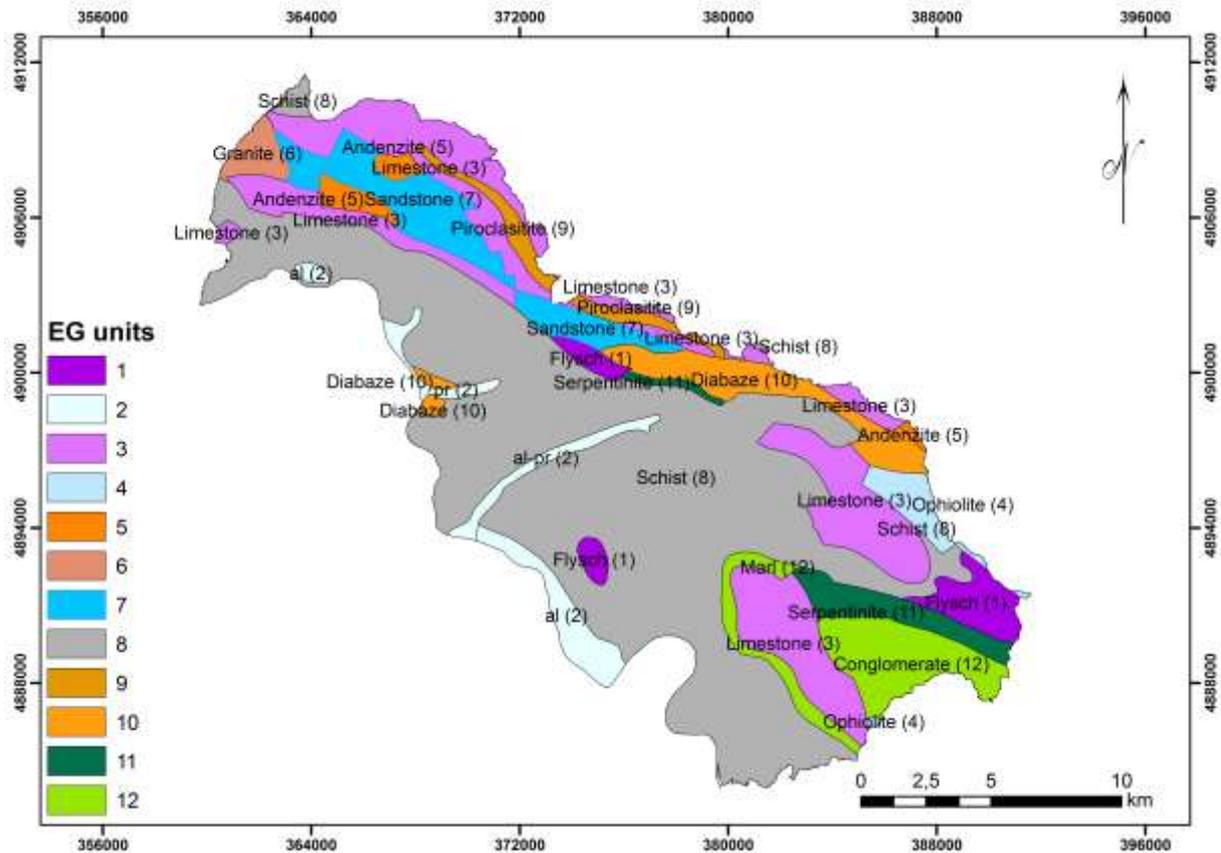
Figure 4. Engineering geological (EG) units of similar mechanical properties TMP.

The EG units are interpreted on the basis of Engineering Geological map. Rock units of similar mechanical properties were aggregated into appropriate complexes. Each complex unit was assigned with an appropriate range of min/max expected values of according strength and triggering parameters. Hydraulic conductivity was used to estimate the T/R ratio. For this purpose, min/max expected values of according strength and triggering parameters. Hydraulic conductivity was used to estimate the T/R ratio. For this purpose, official monthly extreme precipitation (www.hidmet.gov.rs) for Ljubovija was used for estimating critical recharge R. Given that maximal and minimal monthly rainfall equals 394.3 mm and 16.4 mm, respectively, and assuming that T equals hydraulic conductivity, T was recalculated on monthly basis, *i.e.* mm/month, instead of the typical cm/s (see Tab. 1 - Hydraulic conductivity). T was then divided by R giving the respective minimal and maximal T/R. The following EG units, with according adopted parameters, were finally defined (see Tab. 1 - Description).

5. Results

Applying AHP approach first required ranging and scoring of input attributes. All numeric input attributes were separated into five classes with scores 1 to 5.

14

Range intervals for these classes were adjusted according to the landside density within each class. Score 1 suggests that particular class does not contribute to landsliding, while score 5 does. Intermediate scores 2, 3 and 4 are evenly separated intervals between these two extreme classes. Nominal attributes, such

Table 1. Engineering geological units of similar mechanical properties.

EG units	Rock unit	Density [g/cm3]	Cohesion/unit weight [unitless]	Friction angle [°]	Hydraulic conductivity [cm/s]	T/R [unitless]	Description
1	Flysch	1900	0.5–5.5	24–34	0.000001	0.065–1.58	alternating claystone-sandstone sequences, impermeable to superficial recharge, medium-low strength
2	al-pr	1800	0–0.05	21–31	0.01	657.37–15805	gravel-sand-clay soil deposits, very permeable, low strength
3	Limestone	2300	0.5–3	30–58	0.001	65.739–15805	solid rock, permeable, high strength
4	Ophiolite	1800	0.6–3	26–46	0.00001	0.657–15.8	solid rock mixture (chert, sandstone, limestone, diabase), permeable, moderate strength
5	Andenzite	2100	0.3–2	25–47	0.00001	0.657–115.8	solid rock, permeable, moderate strength
6	Granit	2400	0.3–7	25–65	0.000001	0.066–15.8	solid rock, impermeable, high strength
7	Sandstone	1900	0.4–3	20–40	0.00001	0.657–115.8	solid-soft rock, permeable, moderate to low strength
8	Schist	2100	0.4–1.5	20–40	0.000001	0.065–15.8	solid rock, but mantled with clayey crust, relatively permeable, moderate to low strength
9	Piroclasitite	1600	0.8–3	45–65	0.000001	0.065–1.58	soft rock, porous but impermeable, moderate-low strength
10	Diabaze	2300	0.6–5	28–50	0.000001	0.065–1.58	solid rock, impermeable, high strength
11	Serpentinite	2700	0.4–8	60–70	0.000001	0.065–1.58	solid rock, impermeable, high strength
12	Marl	2000	0.6–2	35–55	0.00001	0.065–1.58	soft rock, impermeable, low strength

as A_7 and A_1, did not underwent reclassification by ranging, but some subjective scoring had to be provided. The most difficult was the scoring of the engineering geological units, but two extremes were easily identified: 1 alluvial deposits and

solid intact rock formations, and 5 deluvial deposits and Paleozoic low-crystalline schists. All intermediate classes were scored using the subjective expert judgment. Given these preprocessed inputs, comparison AHP matrix was constructed (Tab. 2). EG units (A_1) were defined as the most important attribute, followed by slope angle A_2, and so forth to erodibility (A_8), which was given the smallest influence on the final model.

Table 2. AHP comparison matrix.

	A_1	A_2	A_3	A_4	A_5	A_6	A_7	A_8
A_1	1.00	1.00	2.00	2.00	4.00	6.00	8.00	9.00
A_2	1.00	1.00	1.00	2.00	3.00	4.00	7.00	8.00
A_3	0.50	1.00	1.00	2.00	3.00	5.00	6.00	7.00
A_4	0.50	0.50	0.50	1.00	2.00	4.00	5.00	7.00
A_5	0.25	0.33	0.33	0.50	1.00	2.00	4.00	6.00
A_6	0.17	0.25	0.20	0.25	0.50	1.00	3.00	5.00
A_7	0.13	0.14	0.17	0.20	0.25	0.33	1.00	3.00
A_8	0.11	0.13	0.14	0.14	0.17	0.20	0.33	1.00
$\sum$	3.65	4.35	5.34	8.09	13.92	22.53	34.33	46.00

After defining relation within different input A_i attributes, matrix normalization was performed (Tab. 3). Each value was divided by the total sum along the column. The result across rows is the eigenvector, which reflects the impact or weight on landslide susceptibility of each attribute (W_{A_i}). Consistency Ratio value $CR = 0.045$ indicated a good and logical pair-wising and scoring of the attributes.

Table 3. Final normalized AHP matrix.

	A_1	A_2	A_3	A_4	A_5	A_6	A_7	A_8	W_{Ai}
A_1	0.27	0.23	0.37	0.25	0.29	0.27	0.23	0.20	0.26
A_2	0.27	0.23	0.19	0.25	0.22	0.18	0.20	0.17	0.21
A_3	0.14	0.23	0.19	0.25	0.22	0.22	0.17	0.15	0.20
A_4	0.14	0.11	0.09	0.12	0.14	0.18	0.15	0.15	0.14
A_5	0.07	0.08	0.06	0.06	0.07	0.09	0.12	0.13	0.08
A_6	0.05	0.06	0.04	0.03	0.04	0.04	0.09	0.11	0.06
A_7	0.03	0.03	0.03	0.02	0.02	0.01	0.03	0.07	0.03
A_8	0.03	0.03	0.03	0.02	0.01	0.01	0.01	0.02	0.02
$\lambda_{max} = 8.445$. $n = 8$. $CR = 0.045$ (< 0.1)									

Superposition of each weighted attribute gives the final additive Landslide Susceptibility Model (LSM) (Fig. 6a). The evaluation was made in comparison with the landslide database (Tab. 4, Fig. 5).

$$LSM = W_{A_1} \times A_1 + W_{A_2} \times A_2 + W_{A_3} \times A_3 + W_{A_4} \times A_4 + W_{A_5} \times A_5 + W_{A_6} \times A_6 + W_{A_7} \times A_7 + W_{A_8} \times A_8$$
$$= 0.26 \times A_1 + 0.21 \times A_2 + 0.20 \times A_3 + 0.14 \times A_4 + 0.08 \times A_5 + 0.06 \times A_6 + 0.03 \times A_7 + 0.02 \times A_8$$

(4)

The *SI* model was prepared based on the spatial aggregation and ranging of strength and triggering parameters. Ranging was performed by readjusting reference values (from various sources) in trial-and-error testing, which was compared against the existing landslide inventory. The inventory was transformed into point features, because the SINMAP extension does not support polygon features input. Plausible parameters adopted as final ones (Tab. 1) were used to construct the final model. Continual *SI* model was further reclassified to standard intervals: 0–0.5 unstable = very high susceptibility, 0.5–1.0 potential instability = high susceptibility, 1.0–1.25 marginally stable = medium susceptibility, 1.25–1.5 stable = low susceptibility, >1.5 unconditionally stable = very low susceptibility (Fig. 6b). For evaluation purposes, pixels with *SI* values <1.0 (first two classes) were aggregated together and compared against landslide instances, whereas pixels with *SI* values ≥1.0 were compared against non-landslide instances of the inventory (Tab. 4).

Table 4. Per-class evaluation of LS models, with adopted metrics.

| Model, class	matching pixels	mismatching pixels	TPrate	FPrate	AUC
AHP model, non-landslide	232093	730	0,603	0,495	
AHP model, landslide	745	152884	0,505	0,397	0.554
SI model, non-landslide	354355	1296	0.996	0.990	
SI-model, landslide	116	12275	0.009	0.003	0.503
RF-1, non-landslide	301479	199	0.783	0.269	
RF-1, landslide	540	83495	0.731	0.217	0.757
RF-2 attributes, non-landslide	270607	150	0.733	0.245	
RF-2 attributes, landslide	589	114367	0.755	0.267	0.750
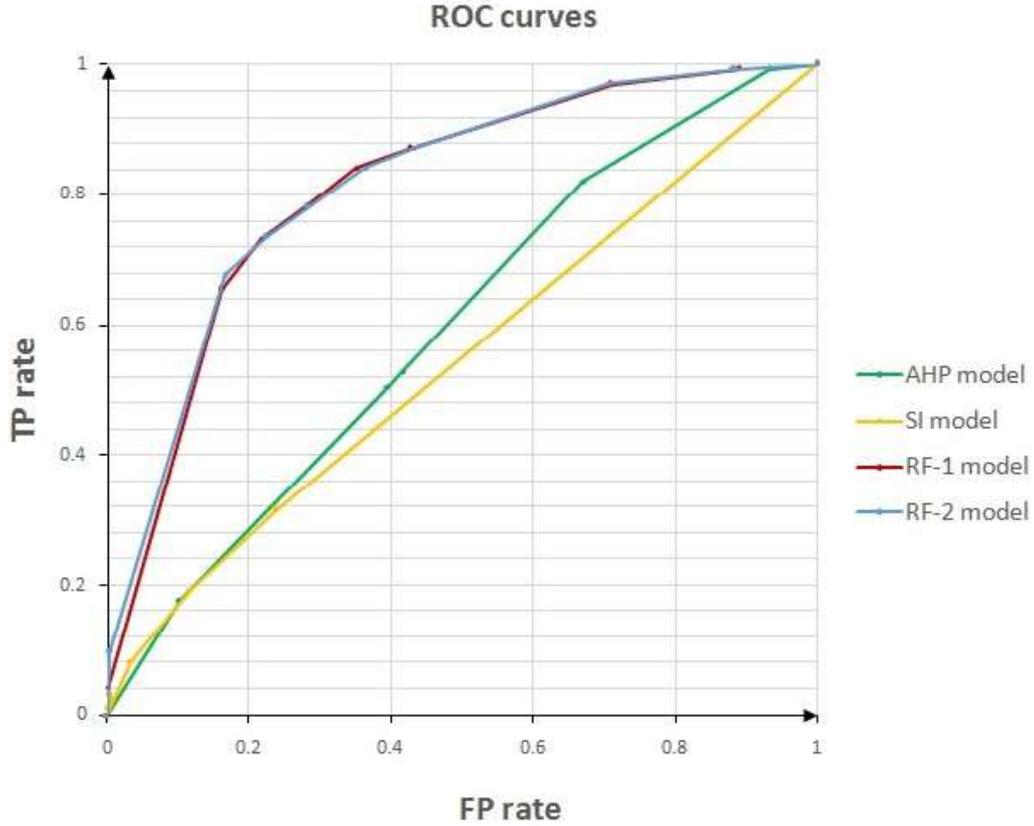
Figure 5. Evaluation of final models presented on ROC curves.

Finally, three basic LSA RF-based models were defined. The first model RF-1, was developed on training and testing datasets that contained all attributes used in AHP based modeling A_{1-8} (Table 2), as well as all conditioning factors used in *SI*-based modeling, *i.e.* 15 attributes. The second RF-2 and third RF-3 models were developed on datasets that contained only attributes A_{1-8} (eight attributes), and SI model parameters (seven attributes), respectively. Furthermore, for each of these three RF based models, the optimal combination of two RF algorithm parameters was defined using the corresponding training dataset and 10-fold cross-validation technique. The range of considered parameters was {100, 250, 500, 1000} for the number of DT in forest, and {2, 3, 4} for the number of randomly used factors, making a total of 12 combinations created for each training dataset, *i.e.* the total number of derived models was 36. These 36 models derived the landslide probability (probability of class 1), for each instance (30x30m cell). In order to further proceed with the landslide susceptibility reclassification and to validate the models, the threshold of 0.75 probability was chosen (based on several trial and error attempts, starting from 0.6, as a logical threshold for very high and high susceptibility combined, to 0.8, as the upper threshold, which is more appropriate for depicting very high susceptibility class only). After the optimal combination of parameters is found, for each of three RF-based models (RF-1, RF-2 and RF-3), the models are validated on the
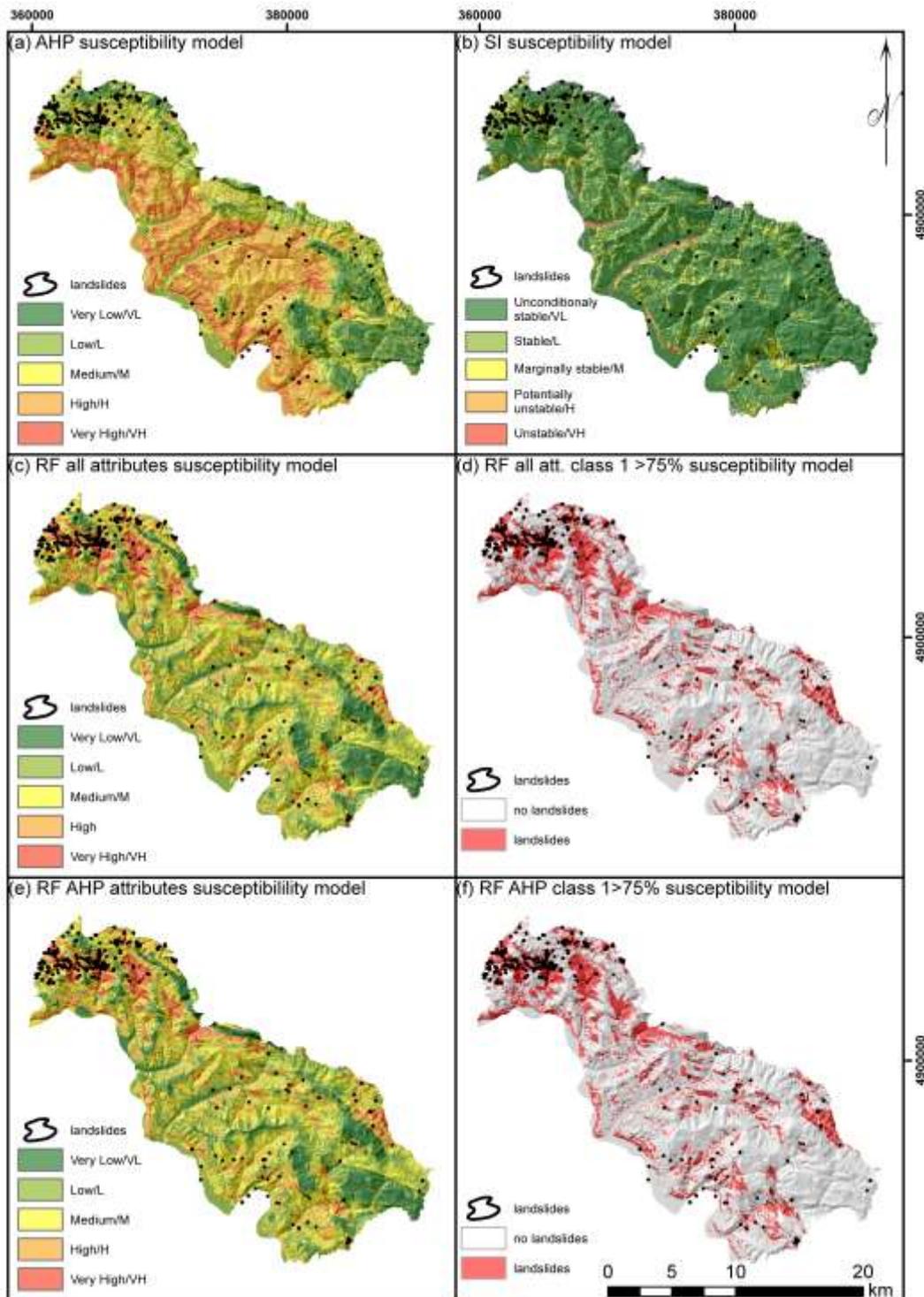
18

Figure 6. Final susceptibility models: (*a*) AHP susceptibility model, (*b*) SI susceptibility model, (*c*) RF-1 all attributes susceptibility model, (*d*) RF-1 All attributes class 1 > 75% susceptibility model, (*e*) RF AHP-2 attributes susceptibility model, (*f*) RF-2 AHP attributes class 1 > 75% susceptibility model.

19

corresponding testing datasets. Considering the value of the defined threshold, only instances with landslide probability greater than 0.75 are declared as landslide and compared against landslide instances from the referent inventory, *i.e.* landslide instances from the corresponding testing datasets.

Since that the main objective of this research is the comparison of the RF, SI, and AHP approach, only the results of two best performing models are presented, *i.e.* RF all attributes susceptibility model – RF1 and RF AHP attributes susceptibility model – RF2 (Tab. 4 and Figs. 6c – 6f).

6. Discussion and conclusion

Evaluation of all models was both qualitative (visual) and quantitative. The metric evaluation was based on the class reclassification, whereby VH and H susceptibility class were compared against landslide inventory. AHP model obviously overestimated Very High and High susceptibility class (too many VH or H areas outside registered landslides), while still failing to map most of the registered landslides into VH or H class (Fig. 6a). Model's performance was relatively poor, with equally balanced false positive and false negative error rates (Tab. 4). It is not particularly reliable, as its AUC is less than 0.6. Visual impression suggests that engineering geological units and Distance to stream chiefly control the distribution of susceptibility classes (as suggested by the AHP matrices), while other factors do not contribute as much. Various variants of AHP model were examined, including even those which gave way to other factors, but the best results were still reached with the presented AHP model. In other words, this is the maximum that was possible to extract from the AHP approach for this particular study.

The *SI* model highly underestimated the VH and H landslide susceptibility classes, *i.e.* FS < 1, as the areal coverage of this class was much smaller than the coverage of the others (Fig. 6b). In addition, VH and H classes fail to map registered landslides, as only 116 / 1412 or 8% of landslide pixels matched. The LS class is too dominant, suggesting that most of the territory is stable, which is false, especially in the North periphery. False Negative rate is too high, together with the True Negative rate. Considering the latter, SI model could seem concurrent to AHP, especially since AUC was also similar (similarly low). However, underestimation of the VH and H susceptibility class definitively disqualifies it. Even though initial hypothesis that landslides triggered in May 2014 where mainly shallow (dismantling of the fragile weathering crusts of Paleozoic schists due to saturation) seemed appropriate and fitting for the initial SI assumptions, it is hereby confirmed the opposite.

The best performing RF model indicates a slight overestimation of VH landslide class, but generally the very good distribution of all VH and H classes across the area in comparison to the landslide inventory. The sampling strategy that was controlling the non-landslide training instances selection by engineering geological criteria was a great improvement, that reduced False Negatives, and False Positives and prevented learning from ambiguous instances. RF models were superior in all aspects (which is obvious on the ROC curves, Fig. 5) particularly TP rates and AUC, over 0.75, which is considerably larger than in previous approaches. As for the comparison between different RF model variants, there was just some slight difference between RF-1 and RF-2 models.

It can be concluded that RF was successful in mapping registered landslides, despite their versatile typology and uneven distribution throughout the area, *i.e.* higher concentration in northern than in the other parts. It is unambiguously superior to expert-driven and deterministic approach, as it succeeds to map landslides where these two approaches fail. Its particular quality is in low FN rates, especially for landslide instances (500–600 VH and H pixels were matching the total of 1412 landslide pixels, which is 30–40%), since FN is more severe error type in LSA.

References

Atkinson, P. M. and Massari, R. (1998): Generalised linear modelling of susceptibility to landsliding in the Central Apennines, Italy, *Comput. Geosci.,* **24**, 373–385, DOI: 10.1016/S0098-3004(97)00117-9.

Ayalew, L. and Yamagishi, H. (2005): The application of GIS-based logistic regression for landslide susceptibility mapping in the Kakuda-Yahiko Mountains, Central Japan, *Geomorphology*, **65**, 15–31, DOI: 10.1016/j.geomorph.2004.06.010.

Barredo, J. I., Benavides, A., Hervás, J. and van Westen, C. J. (2000): Comparing heuristic landslide hazard assessment techniques using GIS in the Tirajana basin, Gran Canaria Island, Spain, *Int. J. Appl. Earth Obs.*, **2**, 9–23, DOI: 10.1016/S0303-2434(00)85022-9.

Bhushan, N. and Rai, K. (2004): *Strategic decision making: Applying the analytic hierarchy process*. Springer, London, 172 pp, DOI: 10.1007/b97668.

Bradley, A. P. (1997): The use of the area under the roc curve in the evaluation of machine learning algorithms, *Pattern Recogn.,* **30**, 1145–1159, DOI: 10.1016/S0031-3203(96)00142-2.

Breiman, L. (1984): *Classification and regression trees.* Chapman and Hall/CRC, 368 pp.

Breiman, L. (2001): Random forests, *Mach. Learn.*, **45**, 5–32, DOI: 10.1023/A:1010933404324.

Cascini, L. (2008): Applicability of landslide susceptibility and hazard zoning at different scales, *Eng. Geol.*, **102**, 164–177, DOI: 10.1016/j.enggeo.2008.03.016.

Catani, F., Lagomarsino, D., Segoni, S. and Tofani, V. (2013): Landslide susceptibility estimation by random forests technique: sensitivity and scaling issues, *Nat. Hazard. Earth Sys.*, **13**, 2815–2831, DOI: 10.5194/nhess-13-2815-2013.

Dai, F. C., Lee, C. F., Li, J. X. Z. W. and Xu, Z. W. (2001): Assessment of landslide susceptibility on the natural terrain of Lantau Island, Hong Kong, *Environ. Geol.*, **40**, 381–391, DOI: 10.1007/s002540000163.

Dahal, R. K. and Hasegawa, S. (2008): Representative rainfall thresholds for landslides in the Nepal Himalaya, *Geomorphology*, **100**, 429–443, DOI: 10.1016/j.geomorph.2008.01.014.

Endrizzi, S., Gruber, S., Dall'Amico, M. and Rigon, R. (2014): GEOtop 2.0: Simulating the combined energy and water balance at and below the land surface accounting for soil freezing, snow cover and terrain effects, *Geosci. Model Dev.*, **7**, 2831–2857, DOI: 10.5194/gmd-7-2831-2014.

Ercanoglu, M., Kasmer, O. and Temiz, N. (2008): Adaptation and comparison of expert opinion to analytical hierarchy process for landslide susceptibility mapping, *B. Eng. Geol. Environ.*, **67**, 565–578, DOI: 10.1007/s10064-008-0170-1.

Fell, R., Corominas, J., Bonnard, C., Cascini, L., Leroi, E. and Savage, W. Z. (2008): Guidelines for landslide susceptibility, hazard and risk zoning for land-use planning, *Eng. Geol.*, **102**, 99–111, DOI: 10.1016/j.enggeo.2008.03.022.

Gavrilović, S. (1971): *Inženjering o bujičnim tokovima i eroziji.* Časopis "Izgradnja", Beograd, 290 pp.

Goetz, J. N., Brenning, A., Petschko, H. and Leopold, P. (2015): Evaluating machine learning and statistical prediction techniques for landslide susceptibility modeling, *Comput. Geosci.,* **81**, 1–11, DOI: 10.1016/j.cageo.2015.04.007.

Guzzetti, F., Carrara, A., Cardinali, M. and Reichenbach, P. (1999): Landslide hazard evaluation: a review of current techniques and their application in a multi-scale study, Central Italy, *Geomorphology*, **31**, 181–216, DOI: 10.1016/S0169-555X(99)00078-1.

Ho, W. (2008): Integrated analytic hierarchy process and its applications – A literature review, *Eur. J. Oper. Res.*, **186**, 211–228, DOI: 10.1016/j.ejor.2007.01.004.

Ishizaka, A., and Labib, A. (2011): Review of the main developments in the analytic hierarchy process, *Expert Syst, Appl,*, **38**, 14336–14345, DOI: 10.1016/j.eswa.2011.04.143.

Komac, M. (2006): A landslide susceptibility model using the Analytical Hierarchy Process method and multivariate statistics in perialpine Slovenia, *Geomorphology*, **74**, 17–28, DOI: 10.1016/j.geomorph.2005.07.005.

Lee, S. (2005): Application of logistic regression model and its validation for landslide susceptibility mapping using GIS and remote sensing data, *Int. J. Remote Sens.*, **26**, 1477–1491, DOI: 10.1080/01431160412331331012.

Lee, S. and Min, K. (2001): Statistical analysis of landslide susceptibility at Yongin, Korea, *Environ. Geol.,* **40**, 1095–1113, DOI: 10.1007/s002540100310.

Lifeng, Y. and Youshui, Z., (2006): Debris flow hazard assessment based on support vector machine, *Wuhan Univ. J. Nat. Sci.,* **11**, 897–900, DOI: 10.1007/BF02830184.

Malczewski, J., Moreno-Sanchez, R., Bojorquez-Tapia, L. A. and Ongay-Delhumeau, E. (1997): Multicriteria group decision-making model for environmental conflict analysis in the Cape Region, Mexico, *J. Environ. Plann. Man.,* **40**, 349–374, DOI: 10.1080/09640569712137.

Marjanović, M., Kovačević, M., Bajat, B. and Voženílek, V. (2011): Landslide susceptibility assessment using SVM machine learning algorithm, *Eng. Geol.*, **123**, 225–234, DOI: 10.1016/j.enggeo.2011.09.006.

Marjanović, M., Vulović, N., Đurić, U. and Božanić, B. (2016): Coupling field and satellite data for an event-based landslide inventory, in: *Proceedings of the 12th International Symposium on Landslides*, 12–19 June, Napoli, Italy, 1361–1366.

Marjanović, M., Samardžić-Petrović, M., Abolmasov, B. and Đurić, U. (2017): Concepts for Improving Machine Learning Based Landslide Assessment, in: *Natural Hazards GIS-based Spatial Modeling Using Data Mining Techniques*, edited by Pourghasemi, H. R. and Rossi, M. Springer (in press).

Montgomery, D. R. and Dietrich, W. E. (1994): A physically-based model for topographic control on shallow landsliding, *Water Resour. Res.,* **30**, 1153–1171, DOI: 10.1029/93WR02979.

Montrasioa, L. and Valentinoa, R. (2016): Modelling rainfall-induced shallow landslides at different scales using SLIP - Part I, *Procedia Engineer.*, **158**, 476–481, DOI: 10.1016/j.proeng.2016.08.475.

Nefeslioglu, H. A., Gokceoglu, C. and Sonmez, H. (2008): An assessment on the use of logistic regression and artificial neural networks with different sampling strategies for the preparation of landslide susceptibility maps, *Eng. Geol.*, **97**, 171–191, DOI: 10.1016/j.enggeo.2008.01.004.

Oh, S. and Lu, N. (2015): Slope stability analysis under unsaturated conditions: Case studies of rainfall-induced failure of cut slopes, *Eng. Geol.*, **184**, 96–103, DOI: 10.1016/j.enggeo.2014.11.007.

Pack, R. T., Tarboton, D. G. and Goodwin, C. N. (2001): Assessing Terrain Stability in a GIS using SINMAP, in: *Proceedings of 15th Annual GIS Conference*, 19–22 February, Vancouver, Canada, 56–68.

Pourghasemi, H. R., Pradhan, B. and Gokceoglu, C. (2012): Application of fuzzy logic and analytical hierarchy process (AHP) to landslide susceptibility mapping at Haraz watershed, Iran, *Nat. Hazards*, **63**, 965–996, DOI: 10.1007/s11069-012-0217-2.

Pradhan, B. (2013): A comparative study on the predictive ability of the decision tree, support vector machine and neuro-fuzzy models in landslide susceptibility mapping using GIS, *Comput. Geosci.*, **51**, 350–365, DOI: 10.1016/j.cageo.2012.08.023.

Rigon, R., Bertoldi, G. and Over, T. M. (2006): GEOtop: A distributed hydrological model with coupled water and energy budgets, *J. Hydrometeorol.*, **7**, 371–388, DOI: 10.1175/JHM497.1.

Saaty, T. L. (1980): *The analytical hierarchy process*. McGraw-Hill, New York.

Saaty, T. L. (1987): The analytic hierarchy process—What it is and how it is used, *Math. Modelling*, **9**, 161–176, DOI: 10.1016/0270-0255(87)90473-8.

Saaty, T. L. and Vargas, L. G. (2001): *Models, methods, concepts and applications of the analytic hierarchy process*. Springer, Kluwer, 333 pp.

Saha, A. K., Gupta, R. P. and Arora, M. K. (2002): GIS-based landslide hazard zonation in the Bhagirathi (Ganga) Valley, Himalayas, *Int. J. Remote Sens.,* **23**, 357–369, DOI: 10.1080/01431160010014260.

Soeters, R. and van Westen, C. J. (1996): Slope instability recognition analysis and zonation, in: *Landslides: Investigation and Mitigation, Special Report No. 247*, edited by Turner, K. T. and Schuster, R. L. Transportation Research Board National Research Council, Washington DC, 129–177.

Subramanian, N., and Ramanathan, R. (2012): A review of applications of Analytic Hierarchy Process in operations management, *Int. J. Prod. Econ.*, **138**, 215–241, DOI: 10.1016/j.ijpe.2012.03.036.

Suzen, M. L. and Doyuran, V., (2004): A comparison of the GIS based landslide susceptibility assessment methods: multivariate versus bivariate, *Environ. Geol.*, **45**, 665–679, DOI: 10.1007/s00254-003-0917-8.

Trigila, A., Iadanza, C., Esposito, C. and Scarascia-Mugnozza, G. (2015): Comparison of Logistic Regression and Random Forests techniques for shallow landslide susceptibility assessment in Giampilieri (NE Sicily, Italy), *Geomorphology*, **249**, 119-136, DOI: 10.1016/j.geomorph.2015.06.001.

Vaidya, O. S. and Kumar, S. (2006): Analytic hierarchy process: An overview of applications, *Eur. J. Oper. Res.*, **169**, 1–29, DOI: 10.1016/j.ejor.2004.04.028.

Vorpahl, P., Elsenbeer, H., Märker, M. and Schröder, B. (2012): How can statistical models help to determine driving factors of landslides?, *Ecol. Model.*, **239**, 27–39, DOI: 10.1016/j.ecolmodel.2011.12.007.

Yalcin, A. (2008): GIS-based landslide susceptibility mapping using analytical hierarchy process and bivariate statistics in Ardesen (Turkey): Comparisons of results and confirmations, *Catena*, **72**, 1–12, DOI: 10.1016/j.catena.2007.01.003.

Yalcin, A., Reis, S., Aydinoglu, A. C. and Yomralioglu, T. (2011): A GIS-based comparative study of frequency ratio, analytical hierarchy process, bivariate statistics and logistics regression methods for landslide susceptibility mapping in Trabzon, NE Turkey, *Catena*, **85**, 274–287, DOI: 10.1016/j.catena.2011.01.014.

Yilmaz, I. (2009): Landslide susceptibility mapping using frequency ratio, logistic regression, artificial neural networks and their comparison: A case study from Kat landslides (Tokat—Turkey), *Comput. Geosci.*, **35**, 1125–1138, DOI: 10.1016/j.cageo.2008.08.007.

SAŽETAK

Usporedba ekspertskog, determinističkog i pristupa Strojnog učenja za ocjenu osjetljivosti na klizišta u općini Ljubovija, Srbija

Jelka Krušić, Miloš Marjanović, Mileva Samardžić-Petrović,
Biljana Abolmasov, Katarina Andrejev i Aleksandar Miladinović

Procjena osjetljivosti na klizišta postaje vrlo produktivno istraživačko područje, pri čemu se prakticiraju različiti pristupi modeliranju kako bi se zonirale visoke i niske vjerojatnosti pojave klizišta. Međutim, ne postoji jasna suglasnost o tome koji je pristup najprikladniji. Razlog nedostatka općeg gledišta na izvedbu različitih pristupa mogao bi se djelomično objasniti osobitostima svake studije. Za procjenu učinkovitosti različitih pristupa neophodno je primjenjivati ih pod istim uvjetima za isto područje istraživanja. U ovome radu su istraživana tri različita pristupa, uključujući ekspertni, deterministički i pristup strojnog učenja, na području općine Ljubovija u zapadnoj Srbiji. Područje je poznato kao osjetljivo na klizišta i predstavlja dobru osnovu za procjenu odabranih metoda. Odlikuje ga kompleksna geologija i sklonost pojavi klizišta koja se obično nalaze u debeloj kori raspadanja paleozojskih formacija sastavljenih od škriljaca i meta-sedimenata. Pod ekstremnim uvjetima za aktivaciju, poput onog koji se odvijao u svibnju 2014., ove debele kore raspadanja se zasićuju i omogućuju raznovrsne pojave klizišta i bujica, na koje ćemo se usredotočiti u ovoj studiji. Primjena ekspertnog pristupa kroz analitički hijerarhijski proces je dala grubu kartu procjene. Deterministički model, koji integrira model beskonačne kosine i hidrološki model, dao je lošije rezultate u usporedbi sa ekspertnom metodom. Ovo se može objasniti time da su pretpostavke korištene u modelu bile previše jednostavne da generički modeliraju takav široki raspon tipologije klizišta. Konačno, pristup strojnog učenja, korištenjem algoritma Random Forest, dao je znatno bolje rezultate i pokazalo se da se može uspješno koristiti s raznovrsnom tipologijom klizišta na većoj prostornoj skali. Njegov AUC učinak je oko 0.75, što je znatno bolje od AUC vrijednosti druga dva modela koji su do 0.55, tj. na razini slučajnog nagađanja.

Ključne riječi: osjetljivost na klizišta, analitička hijerarhija, deterministički model, strojno učenje, Random Forest

Corresponding author's address: Jelka Krušić, Faculty of Mining and Geology, University of Belgrade, Đušina 7, 11 000 Belgrade, Serbia; tel: +381 11 broj broj; e-mail: jelka.krusic@rgf.bg.ac.rs